http://informahealthcare.com/xen
ISSN: 0049-8254 (print), 1366-5928 (electronic)

Xenobiotica

Xenobiotica, 2014; 44(9): 775–784
 DOI: 10.3109/00498254.2014.898808

informa
healthcare

RESEARCH ARTICLE

Identification of UDP-glucuronosyltransferase isoforms responsible for leonurine glucuronidation in human liver and intestinal microsomes

Bo Tan[1]*, Weimin Cai[2]*, Jinlian Zhang[2], Ning Zhou[2], Guo Ma[2], Ping Yang[3], Qing Zhu[1], and Yizhun Zhu[1]

[1]*Department of Pharmacology and* [2]*Department of Clinical Pharmacy, and* [3]*Analytical Center, School of Pharmacy, Fudan University, Shanghai, People's Republic of China*

Abstract

1. Leonurine is a potent component of herbal medicine *Herba leonuri*. The detail information on leonurine metabolism in human has not been revealed so far.
2. Two primary metabolites, leonurine *O*-glucuronide and demethylated leonurine, were observed and identified in pooled human liver microsomes (HLMs) and *O*-glucuronide is the predominant one.
3. Among 12 recombinant human UDP-glucuronosyltransferases (UGTs), UGT1A1, UGT1A8, UGT1A9, and UGT1A10 showed catalyzing activity toward leonurine glucuronidation. The intrinsic clearance (CL_{int}) of UGT1A1 was approximately 15-to 20-fold higher than that of UGT1A8, UGT1A9, and UGT1A10, respectively. Both chemical inhibition study and correlation study demonstrated that leonurine glucuronidation activities in HLMs had significant relationship with UGT1A1 activities.
4. Leonurine glucuronide was the major metabolite in human liver microsomes. UGT1A1 was principal enzyme that responsible for leonurine glucuronidation in human liver and intestine microsomes.

Keywords

Intestine, leonurine, liver, metabolism, microsomes, UDP-glucuronosyltransferases

History

Received 2 January 2014
Revised 20 February 2014
Accepted 24 February 2014
Published online 17 March 2014

Introduction

Leonurine (4-hydroxy-3,5-dimethoxybenzoic acid 4-guanidinobutyl ester) is a potent naturally occurring alkaloid found in the Chinese herb, *Herba leonuri* (HL) (Kong et al., 1976). Over hundreds of years, HL has been widely used in China as a herbal medicine to treat gynaecological disorders including menstrual disorders and dysmenorrhea (Hu, 1976). HL has also been used for the treatment of myocardial ischaemia and blood hyperviscosity (Wang et al., 1988). HL granule is a normal dosage form and its regimen is 10–30 g per person twice or triple a day, in which containing approximately 2.5% leonurine. Since it was first isolated from HL, leonurine has been shown to have uterotonic activity (Sun et al., 2005) and antiplatelet aggregation activity (Sun et al., 2005), and to show cardioprotective (Liu et al., 2009) and neuroprotective (Shi et al., 2011) effects. Using human endothelial cells, leonurine has been shown to have anti-inflammatory properties mediated through inhibition of reactive oxygen species and the NF-κB signalling pathways (Liu et al., 2012a,b). Furthermore, leonurine shows antioxidant activity against ischaemic damage (Loh et al., 2009, 2010) and has been proposed as a protective agent against stroke.

Pharmacokinetic studies have shown that leonurine is rapidly absorbed and has a moderate half-life ($t_{1/2}$) (Li et al., 2013; Zhu et al., 2012b). Following oral administration of leonurine in the rat, the time to reach maximum plasma concentration (T_{max}) and $t_{1/2}$ are 0.95 h and 2.8 h, respectively (Zhu et al., 2012b). However, after oral administration of a high dose (27.2 mg/kg) in rats the maximum plasma concentration (C_{max}) and area under the concentration–time curve (AUC_{0-t}) for leonurine are only 43.3 ng/ml and 75.4 ng/h per ml, respectively (Li et al., 2013). Further studies in our laboratory confirmed that leonurine bioavailability in the rat and dog did not exceed 5.0% and 7.5%, respectively, and found that the plasma concentration of the *O*-glucuronide was much higher than that of leonurine itself in both species (data not shown). Recently, another study reported that the concentration of leonurine *O*-glucuronide is approximately nine-fold higher than that of leonurine in rat plasma, implying extensive metabolism of leonurine *via* glucuronidation (Zhang et al., 2012). To date, however, information on the metabolism of leonurine in human remains unclear.

UDP-glucuronosyltransferases (UGTs) are the most important phase II enzymes and are responsible for metabolizing approximately 40–70% of all clinically used drugs (Wells et al., 2004). The mammalian UGT superfamily comprises four families, denoted UGT1, UGT2, UGT3 and UGT8 (Mackenzie et al., 2005). All UGT families – except

*These authors contributed equally to this work.

Address for correspondence: Yizhun Zhu, Department of Pharmacology, School of Pharmacy, Fudan University, 826 Zhangheng Road, Shanghai 201203, P. R. China. Tel: +86-021-51980008. Fax: +86-021-51980112. E-mail: yizhunzhu@gmail.com

UGT8 – have the capacity to glycosidate both drugs and endogenous compounds. The UGT1 and UGT2 families are mainly responsible for glucuronidation of drugs, using UDP-glucuronic acid (UDPGA) as the sugar donor (Meech et al., 2012). On the basis of gene structure and sequence identity, nine UGT1 members and ten UGT2 members have been identified as functional enzymes in humans (Bock, 2010; Mackenzie et al., 2005). Identification of the human UGT isoform(s) responsible for drug glucuronidation is helpful for elucidating the underlying mechanisms of interindividual variability and the potential for drug–drug interactions (Miners et al., 2010). Moreover, there is recently an increasing interest in interactions between drugs and herbal remedies mediated by UGTs (Chen et al., 2012; Wein et al., 2012). There have been many observations of the effects of components of herbal remedies on drug glucuronidation but the clinical relevance of these interactions needs to be further investigated (Li et al., 2012). For example, quercetin, a flavonoid substrate for UGT1A9 and UGT1A3 that is found in some herbs and food substances, significantly inhibits glucuronidation of mycophenolic acid in human intestinal and liver microsomes (Mohamed & Frye, 2010).

A clear understanding of the metabolism of leonurine and identification of the UGT isoforms involved in its biotransformation is, therefore, important for its clinical use. The aims of this study were (1) to identify the metabolites of leonurine in pooled human liver microsomes (HLMs) and (2) to identify the UGT isoforms responsible for the glucuronidation of leonurine in human liver and intestine using HLMs, human intestine microsomes (HIMs) and recombinant UGTs (rUGTs).

Materials and methods

Chemicals and reagents

Leonurine (purity $\geq$99.8%) was synthesized by ChemPartner Co. Ltd. (Shanghai, China). Leonurine *O*-glucuronide (purity $\geq$99.0%) was biosynthesized in our laboratory as previously reported (Zhang et al., 2012). Bilirubin, atazanavir, propofol, troglitazone, UDPGA, potassium phosphate buffer, magnesium chloride and alamethicin were purchased from Sigma-Aldrich (St. Louis, MO). High-performance liquid chromatography grade acetonitrile and methanol were obtained from Tedia Company, Inc. (Fairfield, OH). Purified water was prepared using a Milli-Q water purification system from Millipore Corporation (Billerica, MA). Pooled mixed gender HLMs ($n = 50$) and HIMs ($n = 10$, from duodenum and jejunum) were available from In Vitro Technologies Co., Ltd (Baltimore, MD). rUGTs (1A1, 1A3, 1A4, 1A6, 1A7, 1A8, 1A9, 1A10, 2B4, 2B7, 2B15 and 2B17), expressed by baculovirus-infected insect cells, were purchased from BD Gentest (Woburn, MA). HLMs from 14 individual East Asian donors were provided by the Research Institute for Liver Diseases (Shanghai) Co., Ltd (Shanghai, China). All other chemicals were of the highest purity available commercially.

Metabolite formation in pooled HLMs

In vitro formation of leonurine metabolites was carried out using pooled HLMs. The incubation mixture contained 0.5 mg protein/ml, 0.1 M potassium phosphate buffer (pH 7.4), 5 mM $MgCl_2$ and 100 μM leonurine in a final volume of 100 μl. The mixture was pretreated with 25 μg/ml alamethicin on ice for 10 min to reduce the latency of UGT activity. After pre-incubating for 5 min at 37 °C, the reaction was initiated by addition of NADPH (5 mM) and UDPGA (8 mM), and then shaken in a water bath at 37 °C for 60 min. The reaction was terminated by the addition of 200 μl of ice-cold acetonitrile. After centrifuging the mixture at 12 000 × *g* for 5 min, the supernatant was collected and dried using a stream of nitrogen at 45 °C. The dried residue was redissolved in 100 μl of mobile phase and a 20 -μl aliquot was analysed by UPLC-UV/MS for metabolite profiling. Incubations without co-factor (NADPH or UDPGA) or without substrate were conducted as negative controls.

Metabolite profiling and identification

Metabolite profiling and structural identification of the samples incubated with HLMs were performed using UPLC-UV/Q-TOF MS. Chromatographic separation was carried out using an Acquity UPLC system (Waters, Milford, MA) with an analytical column (Zorbax SB-C_{18} column, 2.1 × 150 mm, 5 μM; Agilent Technologies Inc., Santa Clara, CA). Separation was achieved using gradient elution as follows: mobile phase, A: 10 mM ammonium acetate with 0.6% acetic acid, B: methanol; gradient elution, 0–2 min: 10% B, 2–12 min: 10% B to 50% B, 12–14 min: 50% B, 14–16 min: 90% B, 16–20 min: 10% B; column temperature, 30 °C; flow rate, 0.3 ml/min; run time, 20 min; UV detection, 278 nM.

MS detection was carried out using a Synapt Q-TOF high-resolution mass spectrometry system (Waters, Milford, MA) operated in positive ion electrospray (ESI) mode. Nitrogen and argon were used as desolvation and collision gases, respectively. The capillary and cone voltages were set at 3.5 kV and 50 V, respectively. The desolvation gas flow was set at 700 l/h at 350 °C. The source temperature was set at 100 °C. The scan range was set at m/z 50–1000. All data were acquired using Lock Spray™ to ensure accuracy and reproducibility. Leucine-enkephalin (m/z 556.2771), at a concentration of 400 ng/ml and a flow rate of 3 μl/min, was used for the lock mass. Data acquisition was performed using an alternating low and elevated collision energy (CE) scan mode (MS^E), which allowed simultaneous acquisition of precursor ion and fragment ion data for all detected analytes in a single run. At low CE, the transfer and trap CEs were 2 and 5 eV, respectively. At high CE, the transfer CE was 15 eV and the trap CE was ramped from 10 eV to 30 eV. Data analysis was performed using MetaboLynx V4.1 software (Waters Corporation), with mass defect filtering (MDF) to reduce interference from the matrix and to facilitate characterization of metabolites (Zhang et al., 2009).

Assay of leonurine glucuronidation in pooled HLMs and HIMs

Using pooled microsomes (HLMs or HIMs), incubation conditions were optimized for linear product formation with respect to microsomal protein concentration (0.1, 0.2 and 0.5 mg/ml) and incubation time (10, 20, 30 and 60 min).

The stock solution of leonurine was prepared in dimethyl sulfoxide (DMSO), and the final concentration of DMSO in the incubations was 0.5%. Preliminary experiments indicated that formation of leonurine *O*-glucuronide was linear up to 30 min of incubation time over the range of microsomal protein concentrations used. Leonurine (0–800 μM) was thus incubated in a final volume of 100 μl containing 0.1 mg/ml of microsomal protein (from HLMs or HIMs), 5 mM $MgCl_2$, 25 μg/ml alamethicin and 100 mM potassium phosphate buffer (pH 7.4). The mixture was kept on ice for 10 min and then preincubated at 37 °C for 3 min. Reaction was initiated by the addition of UDPGA (8 mM) and the sample was then shaken in a waterbath at 37 °C for 15 min. The reaction was terminated by addition of 200 μl of ice-cold acetonitrile containing scopolamine hydrobromide (1 μM) as internal standard (IS). After removal of protein by centrifugation at $12\,000 \times g$ for 5 min, a 5-μl aliquot of supernatant was analysed by LC-MS/MS

Quantification of leonurine *O*-glucuronide

Quantification of leonurine *O*-glucuronide was performed by LC-MS/MS analysis as previously reported (Zhang et al., 2012), with minor revisions. In brief, the HPLC system consisted of an Agilent 1200 series LC system including a degasser, a binary pump, an automatic sampler and a column oven (Agilent Technologies, Santa Clara, CA). A Zorbax SB-C_{18} column (2.1 × 150 mM, 5 μm; Agilent Technologies Inc., Santa Clara, CA) with a column temperature of 30 °C and an eluent flow rate of 0.3 ml/min was used for all separations. The mobile phase was 10 mM ammonium acetate containing 0.6% acetic acid/acetonitrile (80:20, v/v). MS detection was performed with an API 4000 tandem mass spectrometer (AB Sciex, Foster City, CA) used in positive ESI mode. The ion spray voltage was set at 5.0 kV. The source temperature was set at 400 °C. The optimized fragmentation transitions for multiple reaction monitoring (MRM) were m/z 488.3→m/z 312.2 with a CE of 30 eV for leonurine glucuronide and m/z 304.3→m/z 156.3 with a CE of 25 eV for the IS, respectively. Concentrations of leonurine glucuronide in the samples were estimated with $1/x^2$ weighted least-squares regression equations derived from the peak area ratios of leonurine glucuronide to that of the IS. Calibration curves were set up using the biosynthesized standard, leonurine glucuronide, and ranged from 0.01 to 10 μM. Quantification of the analytes was performed using Analyst 1.5 software (AB Sciex, Foster City, CA).

UGT reaction screening

Leonurine was incubated with 12 commercially available recombinant human UGTs (UGT1A1, 1A3, 1A4, 1A6, 1A7, 1A8, 1A9, 1A10, 2B4, 2B7, 2B15 and 2B17), using two substrate concentrations (15 μM and 150 μM) and a constant amount of UGT protein (0.5 mg/ml). Incubations and analyses were carried out as described above (*Assay of leonurine glucuronidation in pooled HLMs and HIMs*). Incubations without UDPGA or without substrate were also carried out to provide negative control samples. Positive controls were conducted in each isoform with incubation of 4-methylumbelliferone (substrates of all UGT1A isoforms except UGT1A4) or trifluoperazine (substrate of UGT1A4) as reported (Uchaipichat et al., 2004).

Enzyme kinetics of glucuronidation in rUGTs

The kinetics of leonurine glucuronidation were examined using UGT1A1, UGT1A8, UGT1A9 and UGT1A10, all of which exhibited significant leonurine glucuronidation activity. Incubation conditions were similar to those described previously (*Assay of leonurine glucuronidation in pooled HLMs and HIMs*). Additional experiments using UGT1A9 were carried out in the presence of bovine serum albumin (BSA; 2%) to avoid the potential inhibitory effects of endogenous substances (Manevski et al., 2012). The incubation samples were analysed by LC-MS/MS.

Chemical inhibition studies

Inhibition studies were conducted using pooled HLMs, pooled HIMs, UGT1A1, UGT1A8, UGT1A9, and UGT1A10 with selective UGT isoform inhibitors or probe substrates. These were atazanavir (0–40 μM), a selective inhibitor of UGT1A1; propofol (0–500 μM), a substrate for UGT1A9; and troglitazone (0–500 μM), a substrate for UGT1A1, UGT1A8 and UGT1A10 (Miners et al., 2010; Shiraga et al., 2012; Watanabe et al., 2002). Leonurine (150 μM) was incubated in the absence or presence of each inhibitor for 15 min at 37 °C, using a protein concentration of 0.1 mg/ml.

Correlation analysis by individual HLMs

Linear regression analysis was used to determine the correlation between the glucuronidation of leonurine and either bilirubin or propofol by microsomes from 14 individual human livers. UGT1A1-catalyzed bilirubin glucuronidation and UGT1A9-catalyzed propofol glucuronidation were assessed by determining rates of metabolite formation as previously reported (Shimizu et al., 2003; Zhou et al., 2010). Reaction mixtures were incubated for 15 min at 37 °C, using 0.1 mg/ml of HLM protein and leonurine, bilirubin, and propofol concentrations of 150 μM, 10 μM and 100 μM, respectively. The protein content in each individual HLMs is provided by the supplier. Correlation analysis was determined by Pearson's product moment method using SPSS 16.0 software (SPSS Inc., Chicago, IL). p Value <0.05 was considered statistically significant.

Data analysis

Kinetic parameters were calculated by nonlinear regression analysis using GraphPad Prism software (GraphPad 5.0 software, Inc., San Diego, CA), with models for either Michaelis–Menten kinetics (Equation (1)) or substrate inhibition kinetics (Equation (2)):

$$V = V_{max} \times S/(K_m + S) \quad (1)$$

$$V = V_{max} \times S/\left(K_m + S + S^2/K_{si}\right) \quad (2)$$

where V is the velocity of the reaction, S is the substrate concentration, K_m is the Michaelis–Menten constant, V_{max} is the maximum velocity, and K_{si} is the substrate inhibition constant. Selection of the appropriate equation for each

dataset was based on the Michaelis–Menten and Eadie–Hofstee plots. The IC_{50}, representing the inhibitor concentration that inhibits 50% of control activity, was determined by non-linear curve fitting using GraphPad Prism software. Kinetic parameters and IC_{50} values are reported as mean ± S.E. from individual duplicates.

Results

Metabolic profiling and identification in pooled HLMs

Metabolites of leonurine in pooled HLMs were identified by the elemental composition of ions obtained from accurate mass measurements, specific MS fragmentation patterns, and/or chromatographic comparison with authentic reference standards. First, the MS fragmentation of leonurine was investigated to facilitate the structural elucidation of the metabolites. Leonurine (labelled as M0) had a retention time of 10.5 min on the HPLC system and showed a protonated molecule ion at m/z 312.1545 on mass spectrometry (Figure 1). Product ions under high CE were observed at m/z 181.0505 ($-C_5H_{13}N_3O$, 100% abundance), 153.0562 ($-C_5H_{13}N_3O$ –CO), 132.1132 ($-C_9H_8O_4$), 114.1024 ($-C_9H_8O_4$ $-H_2O$), 97.0758 ($-C_9H_8O_4$ $-H_2O$ $-NH_3$) and 72.0554 ($-C_9H_8O_4$ $-H_2O$ $-C_3H_6$). Leonurine fragmentation ions were predominantly formed by cleavage of the ester bond (C–O bond) and the guanidinobutyl moiety (Figure 2A).

Using MDF processing, two primary metabolites (labelled as M1 and M2, respectively) were observed in pooled HLMs (Figure 1). Identification of M1 ($[M+H]^+$, m/z 488.1848) as a glucuronic acid conjugate of leonurine was supported by a major fragment ion (also a molecular ion of leonurine) at m/z 312.1546 formed by neutral loss of 176.0302 Da ($-C_6H_8O_6$) (Figure 2B). M1 was confirmed as leonurine *O*-glucuronide by chromatographic and MS comparison with an authentic reference standard. M2 ($[M+H]^+$, m/z 298.1412) was identified as *O*-demethylated leonurine formed by neutral loss of 14.0133 Da ($-CH_2$) compared to the M0 molecular ion (Figure 2C). Since M2 had a similarly characterized product ion (m/z 114.1024) and two demethylated product ions (m/z 167.0334 and m/z 139.0391) compared to the M0 fragment ions, the demethylation site was presumed to be the dimethoxybenzoic acid moiety of leonurine. In contrast to M2, M1 exhibited much higher (approximately 100-fold) mass signal intensity (Figure 1; Table 1). Moreover, in the corresponding UV chromatograms only M1 was detected (Figure 1B).

Leonurine glucuronidation in pooled HLMs and HIMs

The effects of substrate concentration on leonurine glucuronidation were investigated using pooled HLMs and HIMs. As shown using an Eadie–Hofstee plot (Figure 3), leonurine glucuronidation in pooled HLMs was best described by substrate inhibition kinetics. Inhibition effects were apparent at substrate concentrations greater than 600 μM. On the other hand, leonurine glucuronidation in pooled HIMs was best described by the Michaelis–Menten equation (Figure 3). The kinetic parameters for both sources are shown in Table 2. The V_{max} for HIMs was approximately 70% of that for HLMs, and the K_m for HIMs was approximately 1.7-fold higher than that for HLMs, resulting in a 2.3-fold lower value of CL_{int}. Because the K_m values for leonurine glucuronidation by HLMs and HIMs were 133 and 221 μM, respectively, a final concentration of 150 μM leonurine was chosen for all subsequent incubation studies, except for kinetic studies using rUGTs.

UGT reaction screening of leonurine

Glucuronidation of leonurine by 12 commercially available isoforms of human rUGT was measured at two concentrations of leonurine (15 μM and 150 μM). As shown in Figure 4, UGT1A1 exhibited the highest activity, with UGT1A10, UGT1A8 and UGT1A9 displaying very low activities. Other isoforms tested, including UGT1A3, UGT1A4, UGT1A6, UGT1A7, UGT2B4, UGT2B7 and UGT2B17, exhibited negligible or no activity.

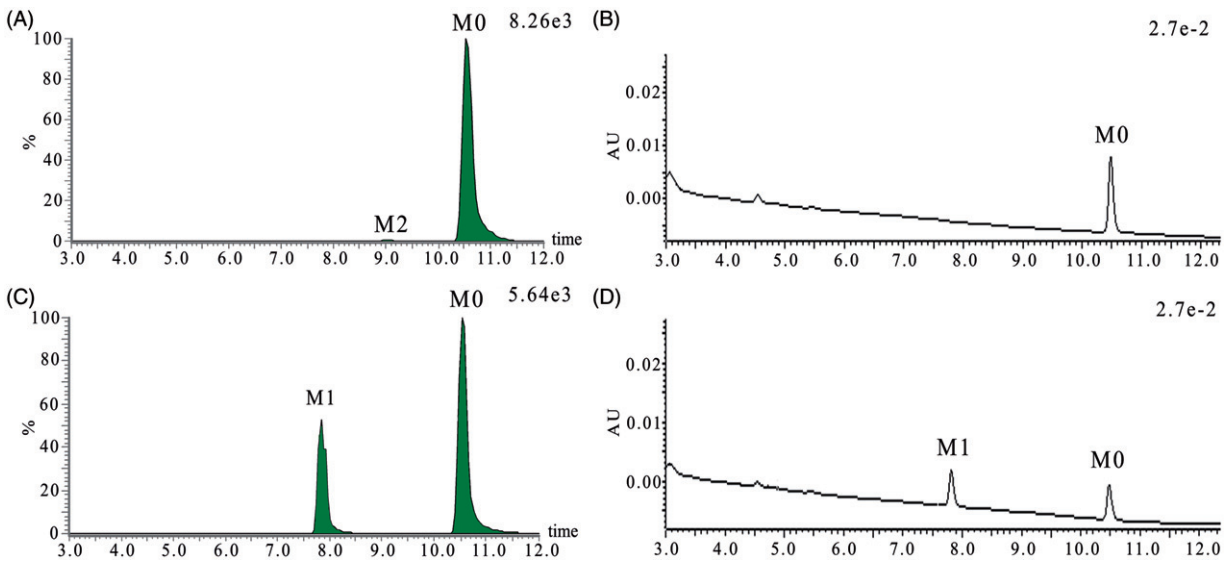

Figure 1. Metabolic profiles of leonurine in pooled HLMs. MDF metabolic profile (A) and UPLC-UV chromatogram (B) for phase I metabolite of leonurine in incubation samples with both NADPH and UDPGA at 37 °C for 60 min.; MDF metabolic profile (C) and UPLC-UV chromatogram (D) for phase II metabolite of leonurine in incubation samples with both NADPH and UDPGA at 37 °C for 60 min.

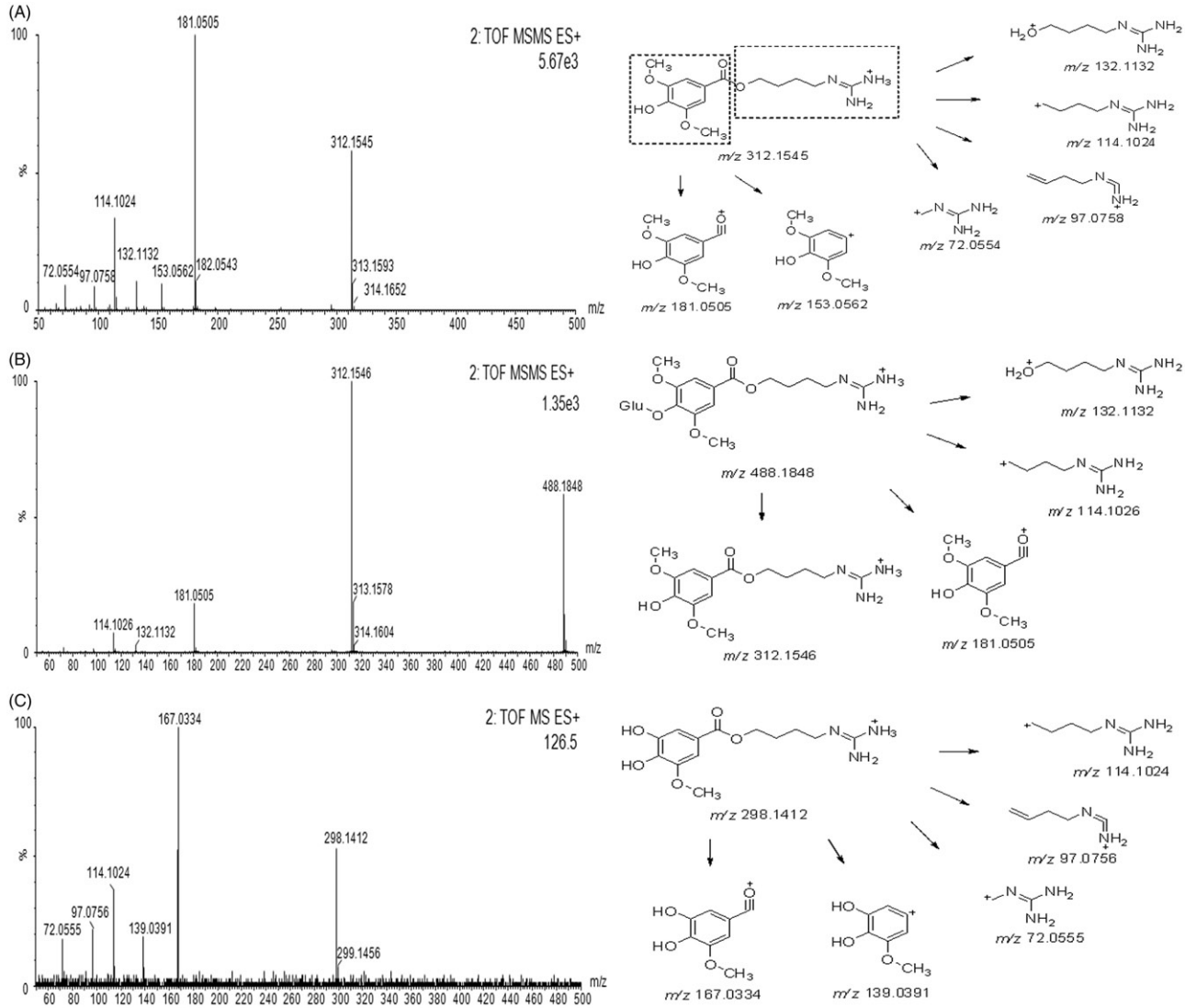

Figure 2. High-collision energy mass spectrum in positive detection mode (obtained on a Q-TOF mass spectrometer) and the proposed fragmentation pathways for leonurine M0 (A), metabolite M1 (B) and metabolite M2 (C), respectively.

Table 1. Identification of leonurine metabolites in pooled HLMs, using UPLC-UV/Q-TOF mass spectrometry.

Name	Metabolite name	m/z $[M+H]^+$	Formula	Error (PPM)	Retention time (min)	Normalized peak area (%)	Fragment ions
M0	Parent	312.1545	$C_{14}H_{21}N_3O_5$	−4.6	10.5	65.9	181.0505, 153.0562, 132.1132, 114.1024
M1	Leonurine *O*-glucuronide	488.1848	$C_{20}H_{29}N_3O_{11}$	−6.6	7.8	33.8	312.1546, 181.0505, 132.1132, 114.1026
M2	*O*-demethylated leonurine	298.1412	$C_{13}H_{19}N_3O_5$	2.9	9.0	0.3	167.0334, 139.0391, 114.1024

Enzyme kinetics for leonurine glucuronidation

Apparent enzyme kinetic parameters for leonurine glucuronidation by four UGT isoforms (UGT1A1, UGT1A8, UGT1A9 and UGT1A10) were estimated using varying concentrations of leonurine (0–800 μM). Incubation conditions were similar for all isoforms. An additional incubation with added BSA (2%) was carried out with UGT1A9 to avoid potential inhibitory effects by endogenous substances (Manevski et al., 2012). The kinetics of glucuronidation by UGT1A1 best fitted the substrate inhibition equation whereas the kinetics of glucuronidation by UGT1A8, UGT1A9 and UGT1A10 best fitted the Michaelis–Menten equation (Figure 5). UGT1A1 showed the highest catalytic activity among the four isoforms (Table 2). Because of the modest solubility of leonurine in aqueous solution, the concentration in the incubation mixtures barely exceeded 800 μM. Thus, the K_m values for UGT1A8 and UGT1A10 were approximations that were close to the maximum concentration (Table 2). As leonurine in 2% BSA showed negligible protein binding ratio (<5%) in the preliminary experiment (data not shown), kinetics of UGT1A9 was calculated without regard to protein binding. UGT1A9 showed different kinetic parameters in the presence or absence of 2% BSA (Table 2). While the V_{max} value slightly increased, the K_m value of UGT1A9 decreased by approximately 50% in the presence of

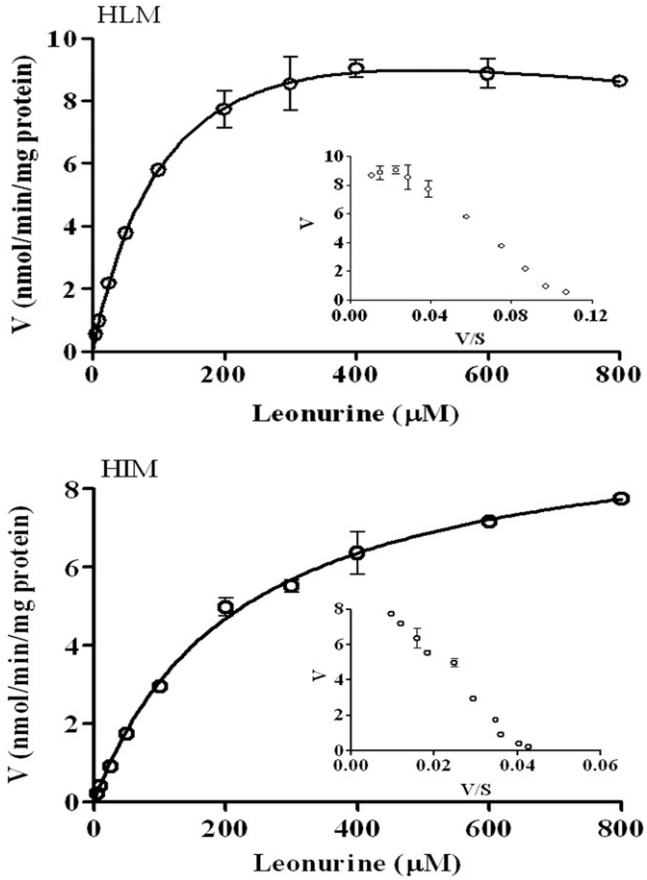

Figure 3. Effects of substrate concentrations on leonurine glucuronidation in pooled HLMs and HIMs. Michaelis–Menten plots and Eadie–Hofstee plots (insets) are shown. Microsomes (0.1 mg of protein/ml) were incubated with 0 to 800 μM leonurine and 8 mM UDPGA at 37 °C for 15 min. Data represent means ± SE of triplicate incubations, and the curves are from model-fitting.

Table 2. Kinetic parameters for leonurine glucuronidation by pooled HLMs, pooled HIMs, and recombinant human UGT isoforms.

Sources	V_{max} nmol/min/mg protein	K_m (μM)	K_{si} (μM)	CL_{int} μl/min/mg protein
HLM[a]	13.8 ± 1.6	133 ± 28	1865 ± 789	104
HIM[b]	9.9 ± 0.4	222 ± 22	N.A.	44.6
UGT1A1[a]	16.2 ± 0.7	98.8 ± 8.5	1281 ± 177	164
UGT1A8[b]	4.2 ± 0.2	514 ± 55	N.A.	8.2
UGT1A9[b]	1.9 ± 0.2	485 ± 66	N.A.	3.9
UGT1A9[b] (BSA)	2.4 ± 0.1	228 ± 20	N.A.	10.5
UGT1A10[b]	6.9 ± 0.6	612 ± 99	N.A.	11.3

N.A., not applicable. BSA, 2% bovine serum albumin was added in incubation mixture.

[a]Kinetic parameters were calculated by substrate inhibition equation (Equation (2)).

[b]Kinetic parameters were calculated by Michaelis–Menten equation (Equation (1)).

BSA. The kinetics of UGT1A9 in the presence of BSA was thus used for comparison with other isoforms. UGT1A9 exhibited the lowest V_{max} value among the four UGTs. Nevertheless, due to its moderate K_m value (228 μM), UGT1A9 exhibited a comparable CL_{int} value to those of UGT1A8 and UGT1A10. Overall, UGT1A1 showed much higher glucuronidation of leonurine (approximately 15- to 20-fold) than UGT1A8, UGT1A9 or UGT1A10.

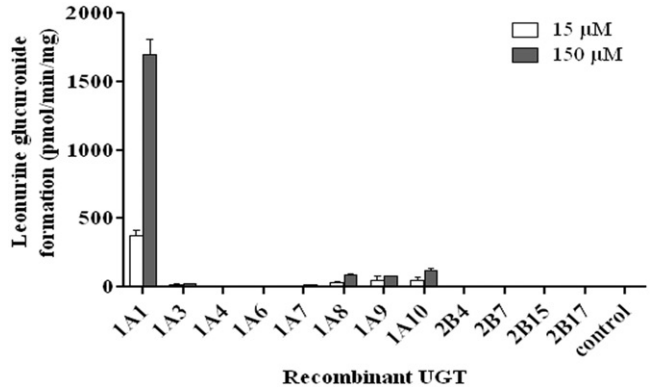

Figure 4. Leonurine glucuronide formation by recombinant human UGTs expressed in baculovirus-infected insect cells. Leonurine (15 or 150 μM) was incubated with each enzyme (0.5 mg/ml) and 8 mM UDPGA at 37 °C for 60 min. Each column represents means ± SE of triplicate incubations.

Inhibition analyses

Inhibition of leonurine glucuronidation by atazanavir, propofol and troglitazone was investigated using pooled HLMs, pooled HIMs, UGT1A1, UGT1A8, UGT1A9 and UGT1A10 (Figure 6). Those compounds showed complete inhibitions toward relevant UGT isoform activity of leonurine at maximum tested concentration. Atazanavir and troglitazone also exhibited strong or medium inhibition of leonurine glucuronidation in HLMs and HIMs. The IC_{50} values of atazanavir were very similar when measured in HLMs, HIMs and UGT1A1 (1.0, 1.0 and 0.9 μM, respectively). At the maximum concentration of atazanavir (40 μM), leonurine glucuronidation by HLMs and HIMs was reduced to 9.7% and 50.0% of control values, respectively. The IC_{50} values of troglitazone in HLMs, HIMs, UGT1A1, UGT1A8 and UGT1A10 were 48.3, 25.4, 56.8, 16.7 and 12.1 μM, respectively. At the maximum concentration of troglitazone (500 μM), leonurine glucuronidation by HLMs and HIMs was reduced to 24.0% and 2.7% of control values, respectively. However, in both HLMs and HIMs, propofol exhibited weak inhibition of leonurine glucuronidation (8.9% and 13.9 % reduction, respectively, compared with control).

Correlation study in HLMs

Leonurine glucuronidation by a panel of 14 individual HLMs was examined at a substrate concentration of 150 μM. The velocity of leonurine glucuronidation ranged from 2.6 to 18.9 pmol/min/mg of protein. Leonurine glucuronidation velocity by the individual HLMs was significantly correlated ($r = 0.909$, $p < 0.001$) with that of the UGT1A1 probe substrate bilirubin, but not correlated ($r = 0.128$, $p > 0.05$) with propofol glucuronidation activity (Figure 7).

Discussion

Leonurine has been administered orally as a component of the herbal medicine, HL, in China for over a hundred years. Recently, leonurine has been proposed as a promising

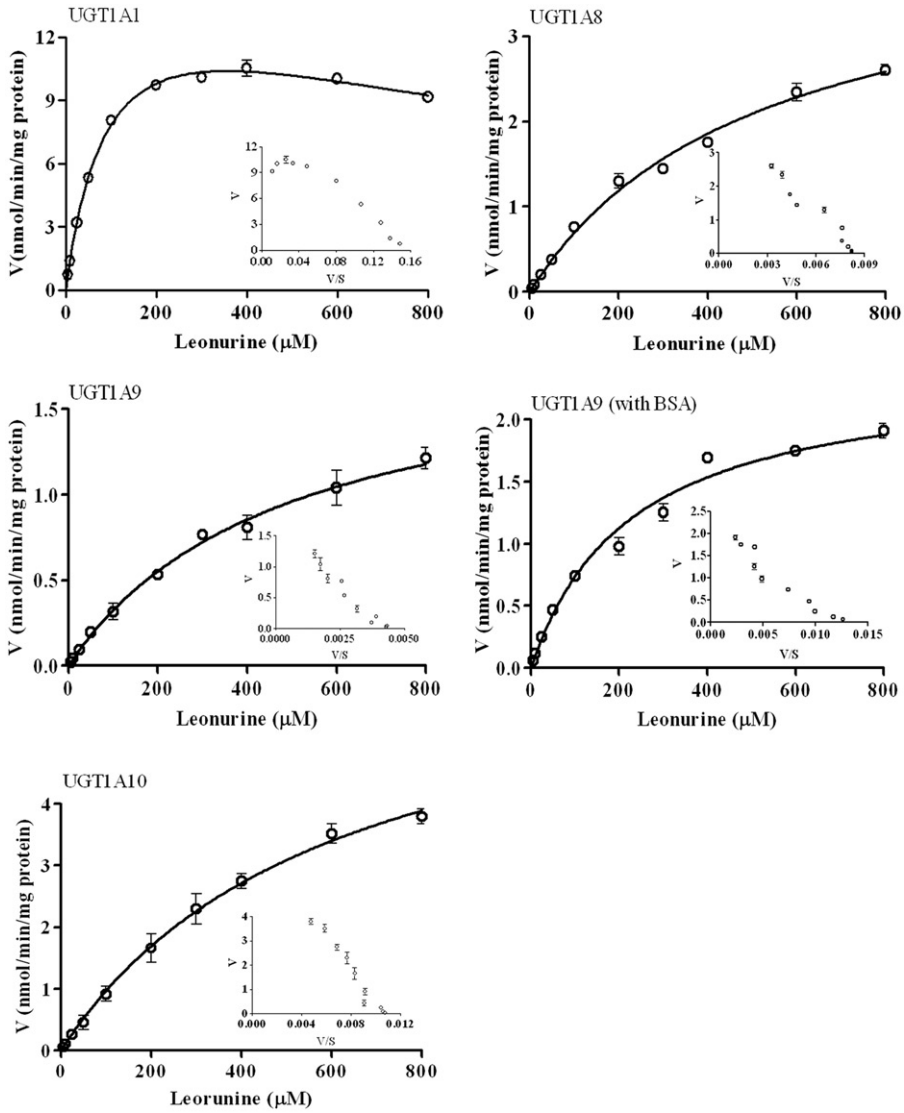

Figure 5. Kinetic analyses of leonurine glucuronidation in recombinant human UGTs. Michaelis–Menten plots and Eadie–Hofstee plots (insets) are shown. Recombinant human UGT isoforms (0.1 mg/ml) were incubated with 0 to 800 μM of leonurine and 8 mM UDPGA at 37 °C for 15 min. Data represent means ± SE of triplicate incubations and curves are from model-fitting.

protective agent against stroke (Loh et al., 2009, 2010). After oral administration of leonurine to rats, the *O*-glucuronide was found to account for 90% of parent drug-related compounds in plasma (Zhang et al., 2012). However, detailed information on leonurine metabolism has not been reported so far. In the present study, we initially carried out a metabolite profiling study of leonurine in pooled HLMs. Two primary metabolites, leonurine *O*-glucuronide and demethylated leonurine, were observed and identified using high resolution mass spectrometry; no secondary metabolites were observed in the study. Leonurine *O*-glucuronide was the major metabolite *in vitro* and was the sole metabolite observed in pooled HLMs using UV detection. This finding was in accordance with a previously reported study in rats (Zhang et al., 2012). The observed metabolism of leonurine in our studies is not unexpected since the molecule contains a phenol group and the majority of phenols are substrates for human UGTs (Ethell et al., 2002). It is likely, therefore, that leonurine *O*-glucuronide is the major metabolite in humans.

The kinetic models of leonurine glucuronidation in pooled HLMs and HIMs were found to be different. As shown by Eadie–Hofstee plots (Figure 3), leonurine glucuronidation in pooled HLMs and HIMs followed substrate inhibition kinetics and typical Michaelis–Menten kinetics, respectively. Compared with HIMs, HLMs exhibited higher capacity and affinity for leonurine glucuronidation; the intrinsic clearance (Cl_{int}) of leonurine by pooled HLMs was 2.3-fold higher than that by HIMs. In humans, microsomal proteins are more abundant in the liver than in the intestine and liver blood flow is greater than intestinal blood flow (Soars et al., 2002), suggesting that the liver may be the main organ involved in leonurine glucuronidation. In the present study, the UGT1 family was found to be almost entirely responsible for glucuronidation of leonurine. Among the 12 recombinant human UGT isoforms, four UGT1 family members (UGT1A1, UGT1A8, UGT1A9 and UGT1A10) were found to be capable of catalysing leonurine glucuronidation, whereas the other UGT isoforms showed minor, or negligible, catalytic activity. Glucuronidation by UGT1A1 followed the same kinetics (substrate inhibition kinetics) as that by HLMs. Moreover, UGT1A1 exhibited the highest catalytic activity; the Cl_{int} of UGT1A1 was approximately 15 - to 20-fold higher than that of UGT1A8, UGT1A9 or UGT1A10 (Table 2). In correlation studies, the leonurine glucuronidation activity of 14 individual HLMs showed significant correlation ($r = 0.909$, $p < 0.01$) with UGT1A1 activities, but little

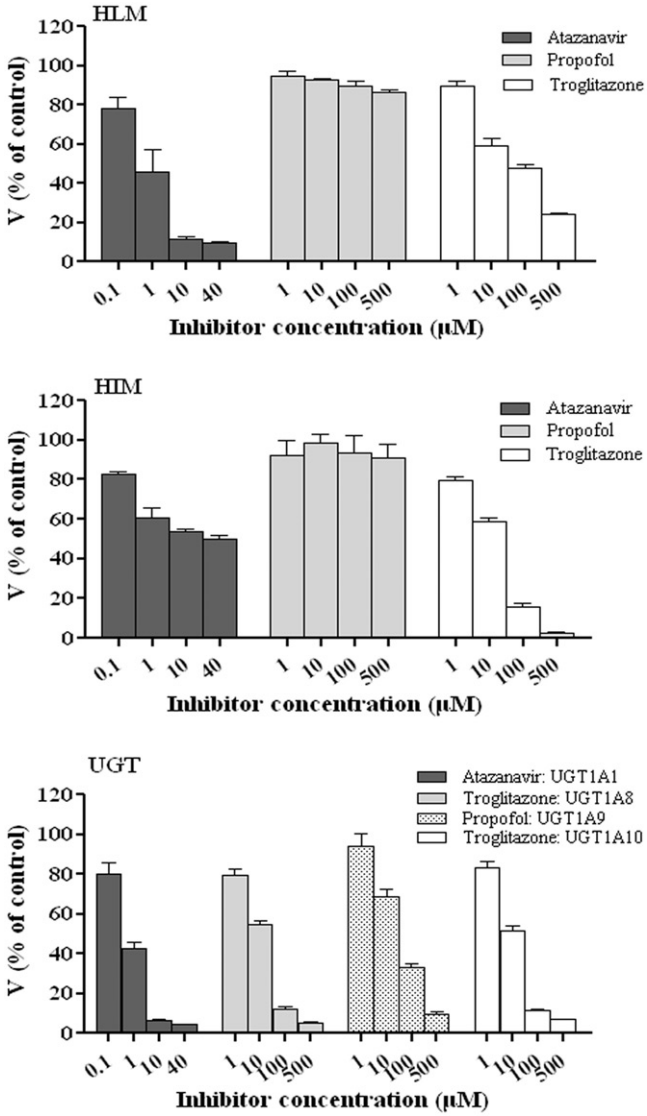

Figure 6. Chemical inhibition of UGT selective inhibitors or typical substrates on leonurine glucuronidation in pooled HLMs, pooled HIMs and several recombinant human UGTs. Leonurine glucuronidation activities were determined using 150 μM of leonurine. Data represent means ± SE of triplicate determinations.

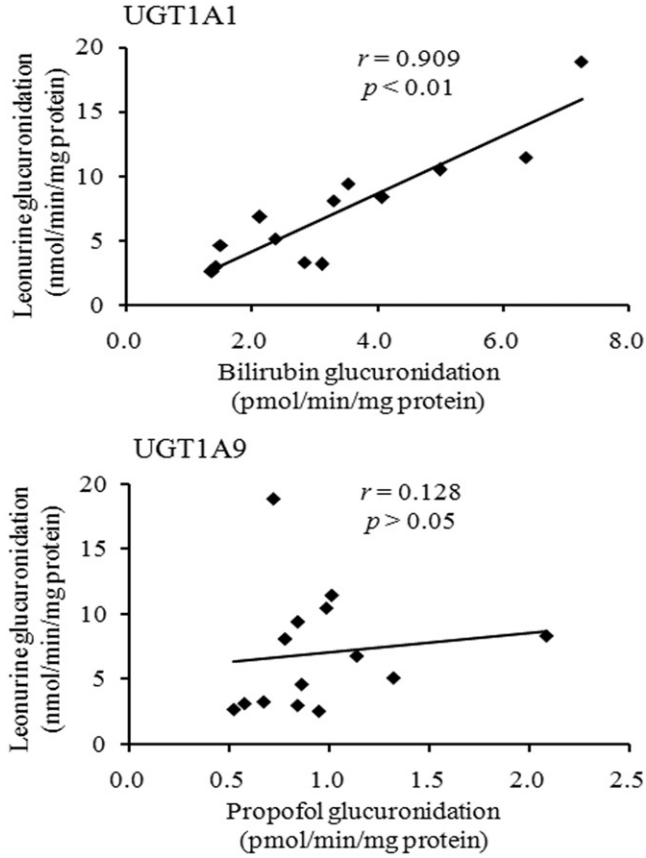

Figure 7. Correlation analysis between leonurine glucuronidation and UGT1A1 (bilibrumglucuronidation) or UGT1A9 (propofol glucuronidation) of specific substrate glucuronidation in microsomes from 14 individual human livers. Leonurine (150 μM) was incubated with microsomes (0.1 mg/ml) for 15 min. Data represent means ± SE of triplicate determinations, and lines are from linear regression analyses.

relationship with UGT1A9 activities ($r = 0.128$, $p > 0.05$). Similar findings were observed in inhibition studies using pooled HLMs. Incubation with the maximum concentration of atazanavir (UGT1A1 inhibitor) or troglitazone (UGT1A1, UGT1A8 and UGT1A10 co-substrate) reduced leonurine glucuronidation activity by pooled HLMs to only 9.7% or 24.0% of the control values, respectively. However, when incubated with propofol, the UGT1A9 substrate, the glucuronidation activity of HLMs remained more than 85% of the control value. These results strongly suggest that UGT1A plays a major role in leonurine glucuronidation in human liver. A correlation study in individual HIMs was not conducted because of the lack of commercial availability of individual human intestine preparations. As shown in Figure 6, the maximum inhibitory effects of atazanavir and troglitazone in pooled HIMs (50.0% versus 97.3%) revealed that UGT1A1 was the major UGT isoform contributing to leonurine glucuronidation in human intestine; UGT1A8 and UGT1A10 may also contribute some extent of the catalytic activity.

Human UGTs are expressed in a tissue-specific manner. According to protein expression levels, UGT1A1 (18.3 pmol/mg) and UGT1A9 (26.7 pmol/mg) are the two most abundantly expressed UGTA1 isoforms in human liver, whereas UGT1A8 and UGT1A10 are not detectable (Fallon et al., 2008; Harbourt et al., 2012). We did not, therefore, carry out correlation and inhibition experiments associated with UGT1A8 or UGT1A10 in HLMs. However, all four UGT1A isoforms that show significant leonurine glucuronidation activity are highly expressed in human intestine. UGT1A1, UGT1A8 and UGT1A9 have similar expression levels that range from 6.1 to 7.2 pmol/mg, whereas UGT1A10 is less abundant (4.7 pmol/mg) (Harbourt et al., 2012). Considering, therefore, protein expression levels of UGTs in human liver and intestine, our study strongly suggests that leonurine glucuronidation in human liver is predominantly catalysed by UGT1A1; in human intestine, the process is also predominantly catalysed by UGT1A1 but UGT1A8 and UGT1A10 also play a smaller role in this tissue.

Among the UGT1A family, UGT1A1 is of particular importance in determining both the safety and efficacy of drug substances (Wells et al., 2004). UGT1A1 catalyses the glucuronidation of a wide variety of drugs and components of

herbal remedies, including some flavonoids (Dong et al., 2012; Kiang et al., 2005; Zhang et al., 2007). Inhibition of UGT1A1 by some components of herbal remedies has also been reported (Mohamed et al., 2010; Zhu et al., 2012a). Additionally, UGT1A1 exhibits high genetic polymorphisms (Canu et al., 2013) and variability in UGT1A1 activity can be linked to clinical outcomes following drug administration. For example, patients who carry a variant *UGT1A1*28* allele have reduced ability to glucuronidate SN-38, the active metabolite of irinotecan, and are at increased risk of severe irinotecan-related toxicity (Tukey et al., 2002). In our study the glucuronidation velocity of leonurine in HLMs showed large individual variation (ranging from 2.6 to 18.9 pmol/min per mg of protein with 65.5% CV) which may be attributed, at least in part, to UGT1A1 polymorphisms. Further studies on gene polymorphisms and the interactions between herbal medicine HL and drugs metabolized by UGT1A1 would thus be of clinical significance.

Conclusions

In summary, UGT1A1 was found to be principally responsible for leonurine glucuronidation in human liver and intestine. Future investigations into the magnitude of UGT1A1-related interactions between drugs, herbal remedies and food substances, together with studies on inter-individual differences in clinical trials would be valuable.

Declaration of interest

The authors declare no conflicts of interests. The authors alone are responsible for the content and writing of this article.

References

Bock KW. (2010). Functions and transcriptional regulation of adult human hepatic UDP-glucuronosyl-transferases (UGTs): mechanisms responsible for interindividual variation of UGT levels. Biochem Pharmacol 80:771–7.

Canu G, Minucci A, Zuppi C, Capoluongo E. (2013). Gilbert and Crigler Najjar syndromes: an update of the UDP-glucuronosyltransferase 1A1 (UGT1A1) gene mutation database. Blood Cells Mol Dis 50:273–80.

Chen XW, Sneed KB, Pan SY, et al. (2012). Herb-drug interactions and mechanistic and clinical considerations. Curr Drug Metab 13:640–51.

Dong RH, Fang ZZ, Zhu LL, et al. (2012). Identification of UDP-glucuronosyltransferase isoforms involved in hepatic and intestinal glucuronidation of phytochemical carvacrol. Xenobiotica 42:1009–16.

Ethell BT, Ekins S, Wang J, Burchell B. (2002). Quantitative structure activity relationships for the glucuronidation of simple phenols by expressed human UGT1A6 and UGT1A9. Drug Metab Dispos 30: 734–8.

Fallon JK, Harbourt DE, Maleki SH, et al. (2008). Absolute quantification of human uridine-diphosphate glucuronosyl transferase (UGT) enzyme isoforms 1A1 and 1A6 by tandem LC-MS. Drug Metab Lett 2:210–22.

Harbourt DE, Fallon JK, Ito S, et al. (2012). Quantification of human uridine-diphosphate glucuronosyl transferase 1A isoforms in liver, intestine, and kidney using nanobore liquid chromatography-tandem mass spectrometry. Anal Chem 84:98–105.

Hu S. (1976). A contribution to our knowledge of Leonurus L., i-mu-ts'ao, the Chinese motherwort. Am J Chin Med 4:219–37.

Kiang TK, Ensom MH, Chang TK. (2005). UDP-glucuronosyltransferases and clinical drug–drug interactions. Pharmacol Ther 106: 97–132.

Kong YC, Yeung HW, Cheung YM, et al. (1976). Isolation of the uterotonic principle from Leonurus artemisia, the Chinese motherwort. Am J Chin Med 4:373–82.

Li B, Wu J, Li X. (2013). Simultaneous determination and pharmacokinetic study of stachydrine and leonurine in rat plasma after oral administration of *Herba Leonuri* extract by LC-MS/MS. J Pharm Biomed Anal 76:192–9.

Li L, Hu H, Xu S, et al. (2012). Roles of UDP-glucuronosyltransferases in phytochemical metabolism of herbal medicines and the associated herb-drug interactions. Curr Drug Metab 13:615–23.

Liu X, Pan L, Wang X, et al. (2012a). Leonurine protects against tumor necrosis factor-alpha-mediated inflammation in human umbilical vein endothelial cells. Atherosclerosis 222:34–42.

Liu XH, Chen PF, Pan LL, et al. (2009). 4-Guanidino-n-butyl syringate (Leonurine, SCM 198) protects H9c2 rat ventricular cells from hypoxia-induced apoptosis. J Cardiovasc Pharmacol 54: 437–44.

Liu XH, Pan LL, Yang HB, et al. (2012b). Leonurine attenuates lipopolysaccharide-induced inflammatory responses in human endothelial cells: involvement of reactive oxygen species and NF-kappaB pathways. Eur J Pharmacol 680:108–14.

Loh KP, Huang SH, Tan BK, Zhu YZ. (2009). Cerebral protection of purified *Herba Leonuri* extract on middle cerebral artery occluded rats. J Ethnopharmacol 125:337–43.

Loh KP, Qi J, Tan BK, et al. (2010). Leonurine protects middle cerebral artery occluded rats through antioxidant effect and regulation of mitochondrial function. Stroke 41:2661–8.

Mackenzie PI, Bock KW, Burchell B, et al. (2005). Nomenclature update for the mammalian UDP glycosyltransferase (UGT) gene superfamily. Pharmacogenet Genom 15:677–85.

Manevski N, Yli-Kauhaluoma J, Finel M. (2012). UDP-glucuronic acid binds first and the aglycone substrate binds second to form a ternary complex in UGT1A9-catalyzed reactions, in both the presence and absence of bovine serum albumin. Drug Metab Dispos 40: 2192–203.

Meech R, Miners JO, Lewis BC, Mackenzie PI. (2012). The glycosidation of xenobiotics and endogenous compounds: versatility and redundancy in the UDP glycosyltransferase superfamily. Pharmacol Ther 134:200–18.

Miners JO, Mackenzie PI, Knights KM. (2010). The prediction of drug-glucuronidation parameters in humans: UDP-glucuronosyltransferase enzyme-selective substrate and inhibitor probes for reaction phenotyping and in vitro–in vivo extrapolation of drug clearance and drug–drug interaction potential. Drug Metab Rev 42: 196–208.

Mohamed MF, Frye RF. (2010). Inhibition of intestinal and hepatic glucuronidation of mycophenolic acid by Ginkgo biloba extract and flavonoids. Drug Metab Dispos 38:270–5.

Mohamed MF, Tseng T, Frye RF. (2010). Inhibitory effects of commonly used herbal extracts on UGT1A1 enzyme activity. Xenobiotica 40: 663–9.

Shi XR, Hong ZY, Liu HR, et al. (2011). Neuroprotective effects of SCM198 on 6-hydroxydopamine-induced behavioral deficit in rats and cytotoxicity in neuronal SH-SY5Y cells. Neurochem Int 58: 851–60.

Shimizu M, Matsumoto Y, Tatsuno M, Fukuoka M. (2003). Glucuronidation of propofol and its analogs by human and rat liver microsomes. Biol Pharm Bull 26:216–19.

Shiraga T, Yajima K, Suzuki K, et al. (2012). Identification of UDP-glucuronosyltransferases responsible for the glucuronidation of darexaban, an oral factor Xa inhibitor, in human liver and intestine. Drug Metab Dispos 40:276–82.

Soars MG, Burchell B, Riley RJ. (2002). In vitro analysis of human drug glucuronidation and prediction of in vivo metabolic clearance. J Pharmacol Exp Ther 301:382–90.

Sun J, Huang SH, Zhu YC, et al. (2005). Anti-oxidative stress effects of *Herba leonuri* on ischemic rat hearts. Life Sci 76:3043–56.

Tukey RH, Strassburg CP, Mackenzie PI. (2002). Pharmacogenomics of human UDP-glucuronosyltransferases and irinotecan toxicity. Mol Pharmacol 62:446–50.

Uchaipichat V, Mackenzie PI, Guo XH, et al. (2004). Human udp-glucuronosyltransferases: isoform selectivity and kinetics of 4-methylumbelliferone and 1-naphthol glucuronidation, effects of organic solvents, and inhibition by diclofenac and probenecid. Drug Metab Dispos 32:413–23.

Wang ZS, Li DW, Xia WJ, et al. (1988). The therapeutic effect of *Herba leonuri* in the treatment of coronary myocardial ischemia. J Tradit Chin Med 8:103–6.

Watanabe Y, Nakajima M, Yokoi T. (2002). Troglitazone glucuronidation in human liver and intestine microsomes: high catalytic activity of UGT1A8 and UGT1A10. Drug Metab Dispos 30:1462–9.

Wein S, Cermak R, Wolffram S, Langguth P. (2012). Chronic quercetin feeding decreases plasma concentrations of salicylamide phase II metabolites in pigs following oral administration. Xenobiotica 42: 477–82.

Wells PG, Mackenzie PI, Chowdhury JR, et al. (2004). Glucuronidation and the UDP-glucuronosyltransferases in health and disease. Drug Metab Dispos 32:281–90.

Zhang H, Zhang D, Ray K, Zhu M. (2009). Mass defect filter technique and its applications to drug metabolite identification by high-resolution mass spectrometry. J Mass Spectrom 44:999–1016.

Zhang J, Liu H, Mao Y, et al. (2012). Toxicokinetics of leonurine and its metabolite in rats. Chin J Pharm 43:451–4.

Zhang L, Zuo Z, Lin G. (2007). Intestinal and hepatic glucuronidation of flavonoids. Mol Pharm 4:833–45.

Zhou J, Tracy TS, Remmel RP. (2010). Bilirubin glucuronidation revisited: proper assay conditions to estimate enzyme kinetics with recombinant UGT1A1. Drug Metab Dispos 38:1907–11.

Zhu L, Ge G, Liu Y, et al. (2012a). Potent and selective inhibition of magnolol on catalytic activities of UGT1A7 and 1A9. Xenobiotica 42: 1001–8.

Zhu Q, Cai WM, Sha XY, et al. (2012b). Quantification of leonurine, a novel potential cardiovascular agent, in rat plasma by liquid chromatography-tandem mass spectrometry and its application to pharmacokinetic study in rats. Biomed Chromatogr 26:518–23.